Gold/Tin Oxide Nanocomposite by Nanojoining

Geetika Bajaj and R.K. Soni[*]

Department of Physics, Indian Institute of Technology Delhi, New Delhi-110016, India

Abstract: In this paper we report synthesis of Au-SnO$_2$ nanocomposite by nano-joining. It involves synthesis of Au and SnO$_2$ colloids separately followed by post irradiation of mixed Au-SnO$_2$ colloids. We have used 532 nm and 1064 nm wavelengths of a pulsed Nd:YAG laser and different post irradiation time. The post irradiation by 532 nm laser light results in formation of Au-SnO$_2$ nanocomposite by nanojoining. Distinct gold nanoparticles along with the SnO$_2$ aggregates are observed in case of post irradiation by 1064 nm showing no nanojoining effect. Our results indicate that nanojoining is a wavelength selective process. The X-ray Photoelectron Spectroscopy (XPS) indicates negative binding energy shift of Au 4f peak whereas the position of Sn 3d peak remains unaffected after the post irradiation process. The invariance of Sn 3d peak after post irradiation indicates no change in the valence state of Sn. A red shift with respect to the plasmon resonance peak of gold colloids is observed in Au-SnO$_2$ nanocomposite.

PACS: 52.38.Mf; 61.46.-w; 81.07. –b.

INTRODUCTION

The nanocomposite materials synthesis has gained considerable attention from material scientists because various physical properties can be tailored in these nanocomposites systems for specific applications. The field of nanocomposite materials has been widely recognized as one of the most promising and rapidly emerging research areas. The constituents of a nanocomposite have different structures, compositions and properties. Thus, the materials built from them can be multifunctional. The single component building blocks with dimensions in the nanometer size make it possible to design and create new materials with unprecedented flexibility. Recent reports have shown that these nanocomposites materials offer enhanced properties and improved characteristics as compared to their single components counterpart materials [1-4]. Apart from the properties of individual components in a nanocomposite, interfaces can also play an important role in enhancing or limiting the overall properties of the system.

The immense potential of Au-SnO$_2$ nanocomposite in a broad range of applications has recently created a lot of interest in this material system. They can be used as nanocapacitors with high electronic capacitance and low leakage rates [5]. They are used for efficient catalytic activity [6] and for sensor applications [7]. Recently, pulsed laser ablation in liquid (PLAL) has been widely applied for the generation of nanoparticles (NPs). PLAL has proved to be an efficient and versatile physical method for fabrication of nanomaterials [8]. It offers many advantages over the conventional wet chemical methods for synthesis of colloidal NPs. In comparison to wet chemical techniques, in which the

synthesized NPs are significantly surface contaminated and require secondary treatments, PLAL is a chemically clean synthesis process. It is capable of generating NPs in the form of colloidal without the formation of chemical by-products. This technique possesses flexibility in controlling the properties of NPs by appropriate choice of laser parameters [9, 10] and surrounding liquid [10, 11].

In this paper, we have studied the structural, compositional and optical properties of Au-SnO$_2$ nanocomposites obtained by two-step method. At first, laser ablation of pure single metal targets is performed in deionized water to form individual gold and tin oxide colloidal. The two colloidal solutions are mixed and post irradiated by pulsed laser beam to form Au-SnO$_2$ nanocomposite by nanojoining effect. The nanojoining involves selective heating and melting of one of the components by using 532 nm laser wavelength in a mixed colloidal solution whereas the other component remains unaffected in the post irradiation [12]. The heated or melted gold particles can join at the interface with SnO$_2$ NPs which are relatively at lower temperature.

EXPERIMENTAL

A gold target (99.9% pure) immersed in 10 cm^3 of deionized water was kept in a glass vial. The gold target was irradiated with the second harmonic of a pulsed Nd:YAG laser (532 nm) with pulse repetition rate 10 Hz and pulse width 5 ns. The laser beam was focused on the target surface using a lens of focal length 150 mm. The ablation was carried out for 15 minutes with laser energy 36 mJ/pulse. A tin target (99.9%) immersed in 10 cm^3 of deionized water was ablated separately for 30 minutes by the same laser at a lower energy 18 mJ/pulse. The lower laser energy was used for ablation of tin owing to lower melting point of tin as compared to gold. The synthesized Au and SnO$_2$ colloidal solution were then mixed and post irradiated by fundamental (1064 nm) or second harmonic (532 nm) wavelength light of

*Address correspondence to this author at the Department of Physics, Indian Institute of Technology Delhi, New Delhi-110016, India;
Tel: +91 1126591304; Fax: +91 1126581114;
E-mail: ravisoni@physics.iitd.ac.in

Nd:YAG laser at the energy of 14 mJ/pulse for 10 min. The suspensions were dropped on copper mesh covered with an amorphous carbon film and dried at room temperature for transmission electron microscopy (TEM) measurements. For compositional analysis of the synthesized nanocomposite, the sample was centrifuged and the collected powder was dried on a quartz substrate for X-ray Photoelectron Spectroscopy measurements using SPECS XPS system attached with PHOIBOS. The survey scan was obtained at a step size 1eV. The samples were sputtered using Ar ion beam of energy 5 keV for 2 min. The HRXPS of photoelectron peaks of main elements was then obtained at a step size of 0.05 eV. The relative peak shifts due to the electrostatic charge-up were corrected by fixing the peak position of the carbon (C1s peak) at 284.6 eV. The optical absorption of the samples was recorded using Perkin Elmer Lambda 35 spectrometer with resolution of 1 nm.

RESULTS AND DISCUSSION

The gold NPs are prepared by pulsed laser ablation of gold target in deionized water. The solution turned red after the ablation of gold target. The formation of gold colloidal is confirmed by appearance of characteristic plasmon peak at 520 nm in the absorption spectrum (discussed later). The tin oxide NPs are prepared by pulsed laser ablation of tin target in deionized water. The solution remained colorless but appeared turbid after the ablation process. The formation of tin oxide NPs can be explained on the basis of pulsed laser induced reactive quenching in liquid medium [13]. In case of laser ablation of transition metal targets the surrounding liquid not only confines the ablated species at the liquid–solid interface but also acts as a mediator for chemical reaction at the liquid–solid interface. Strong chemical reactions can occur between the highly energetic species ablated from the target and the surrounding liquid molecules. The tin oxide NPs can be formed by the chemical reaction between active tin species and water molecules.

After the formation of Au and SnO_2 colloids, we mixed the colloids in equal volumetric ratio and post irradiated with 1064 nm or 532 nm wavelength of Nd:YAG laser. The TEM micrographs of the samples are shown in Fig. (**1**). The pH value of the oxide NPs in pure water is below the isoelectric point indicating that the particles are positively charged at the surface [13]. We have carried out ablation in the absence of any surfactant so the positively charged NPs initially repel each other due to electrostatic repulsive forces. The repulsive forces promote further oxidation by attachment of the hydroxyl which causes decrease in surface charge. Due to reduced surface charge the tin oxide NPs can coalesce to form SnO_2 aggregates. The TEM images of samples post irradiated by 1064 nm laser wavelength showed distinct gold NPs in between the SnO_2 aggregates. In case of the samples post irradiated by 532 nm laser wavelength, change in particle morphology was observed in TEM micrographs. From the TEM micrographs, it is evident that the molten gold NPs have joined with SnO_2 NPs to form of Au-SnO_2 nanocomposite by nano-joining. The elongated rod like structure clearly shows the nano-joining effect. From the TEM micrographs it can be concluded that after post irradiation by 1064 nm the particles remain distinct and no nano-joining effect was observed. The post irradiation by

532 nm, on the other hand, results in formation of Au-SnO_2 nanocomposite by nano-joining and clearly shows the wavelength selective nature of the joining process. In case of post irradiation by 532 nm wavelength, strong laser light interaction with gold NPs can occur. The gold NPs in mixed solution absorb photons efficiently as the laser wavelength is near the plasmon absorption band. The melting point of gold NPs decreases with decrease in particle size and is sufficiently less in comparison of bulk gold [14]. During a single laser pulse, one gold NP is considered to absorb many photons successively and the temperature reaches as high as the melting point [15]. Thus absorption of photons can lead to heating and even melting of gold NPs. The selective heating of the gold NPs due to near resonance condition with surface plasmon absorption (SPA) band around 520 nm creates liquid suspension in the solution during the post irradiation process. The heating effect of the tin oxide NPs in solution is relatively weak due to extremely low absorption in the visible range. Tin oxide is wide bandgap (3.6 eV) semiconductor and its band edge absorption occurs at 345 nm which blue shifts in nanoparticles due to reduced size effect. The tin oxide nanoparticles show strong absorption in UV range and have extremely weak absorption in visible range. The tin oxide NPs remain in solid form during the laser irradiation. The liquid gold suspension in the colloidal solution joins the solid tin oxide NPs resulting in the formation of Au-SnO_2 nanocomposite [12]. For the samples prepared by post irradiation by 1064 nm laser wavelength, the joining effect was weak owing to weak absorption of both Au NPs and SnO_2 NPs at this wavelength.

The effect of post-irradiation time on the morphology of the Au-SnO_2 nanocomposites was investigated by TEM. The TEM micrographs of the Au-SnO_2 nanocomposites are shown in Fig. (**2**). The Au-SnO_2 nanocomposites synthesized using 532 nm showed a drastic change in particle morphology from spherical to elongated nanoparticles with increasing post-irradiation time. For post-irradiation time of 5 min the particles are mostly spherical in shape with an average particle size of 4 nm and are interconnected. We observe a change in circularity with an increase in irradiation time. For the post irradiation time of 10 mins some spherical nanoparticles with an average size of about 7 nm were observed along with the elongated particles. The length of these elongated particles varies from 8 nm to 26 nm. The nano-joining process is size selective in nature. The melting point of gold nanoparticles decreases appreciably with decrease in the particle size due to reduction in coordination number and cohesive energy of the surface atoms. During the post-irradiation process, the smaller nanoparticle can undergo complete melting whereas the larger particle undergo only partial melting or surface melting which indicates that the smaller particles have a stronger role in this process. Fig. (**2**) shows increased average particle size with increase in post-irradiation time due to laser induced thermal fusion of smaller particles. The change in morphology with increase post-irradiation time can be explained on the basis of fusion of photo-thermally melted gold nanoparticles. The particles can undergo either photo-thermal fusion or photo-fragmentation depending upon their state before irradiation. During the post-irradiation process the temperature of gold nanoparticles can reach much above the melting point and
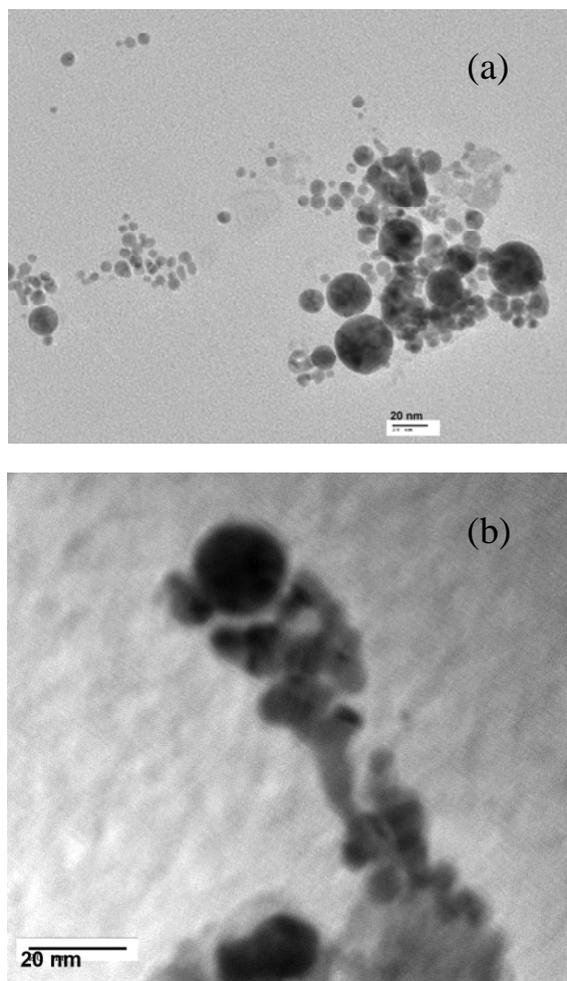
Fig. (1). High magnification TEM micrographs of the samples post irradiated at laser energy of the 14 mJ/pulse for 10 min by (**a**) 1064 nm (**b**) 532 nm.

the heated particles can fuse together by encounter and coagulation. The initial agglomeration may enhance the intrinsic encounter rate of the nanoparticles. The laser induced fusion of these aggregates form larger particles on irradiation.

The XPS spectrum of the synthesized tin oxide NPs and Au-SnO$_2$ nanocomposite are shown in Fig. (**3**). The HRXPS of Au 4f and Sn 3d peak is shown in insets. The spectrum of tin oxide shows the photoelectron peaks of Sn, O, C, and weak Si peaks which came from the quartz substrate. The Sn3d$_{5/2}$ peak was located at 486.6 eV which corresponds to the binding energy of Sn in SnO$_2$ [16]. The XPS spectrum of the Au-SnO$_2$ nanocomposite shows that the photoelectron peaks of Au, Sn, O, C, and weak Si peaks which came from the quartz substrate. The Sn3d$_{5/2}$ peak was located at 486.55 eV position. The invariance in Sn 3d peak positions shows that no change in the oxidation state of tin has occurred after the post irradiation process. It also confirms the fact that post irradiation process resulted in nano-joining and not in partial alloying of Au and SnO$_2$ NPs.

The 4f$_{7/2}$ peak in Au-SnO$_2$ nanocomposite was located at 83 eV. The Au 4f peak show a binding energy negative shift of 1 eV with respect to bulk Au (84 eV). The binding energy of Au 4f peaks strongly depends on the chemical or electronic environment surrounding it. The shift of Au 4f binding energy can be ascribed to the small size of Au NPs (< 2 nm) or to the electron structure difference between metal and the support [17]. In our case, the charge transfer from the SnO$_2$ can be responsible for the observed negative shift. The difference in the work function of Au (5.42 eV) [18] and SnO$_2$ (4.3 eV) [19] facilitates the electron transfer from SnO$_2$ to Au [20] and the negative charging leads to the shift toward lower binding energies as compared to bulk gold.

The absorption spectra of the synthesized gold NPs, tin oxide NPs, Au-SnO$_2$ nanocomposite samples prepared by
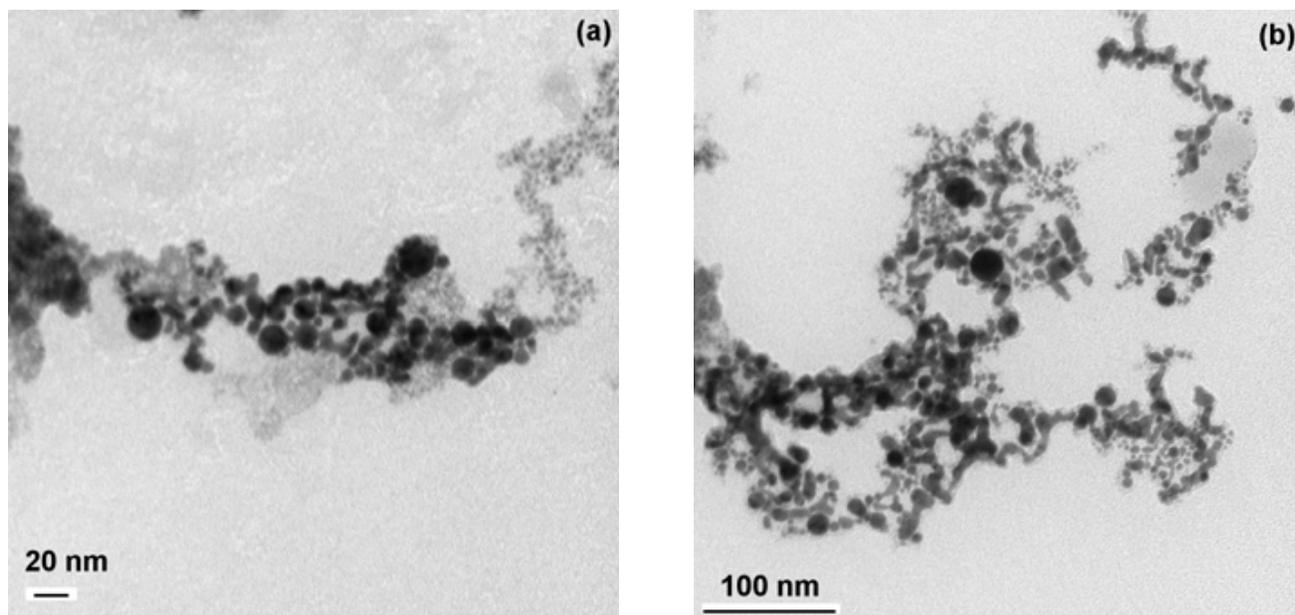

Fig. (2). TEM micrographs of the synthesized samples post-irradiation by 532 nm for time (**a**) 5 min and (**b**) 10 min.
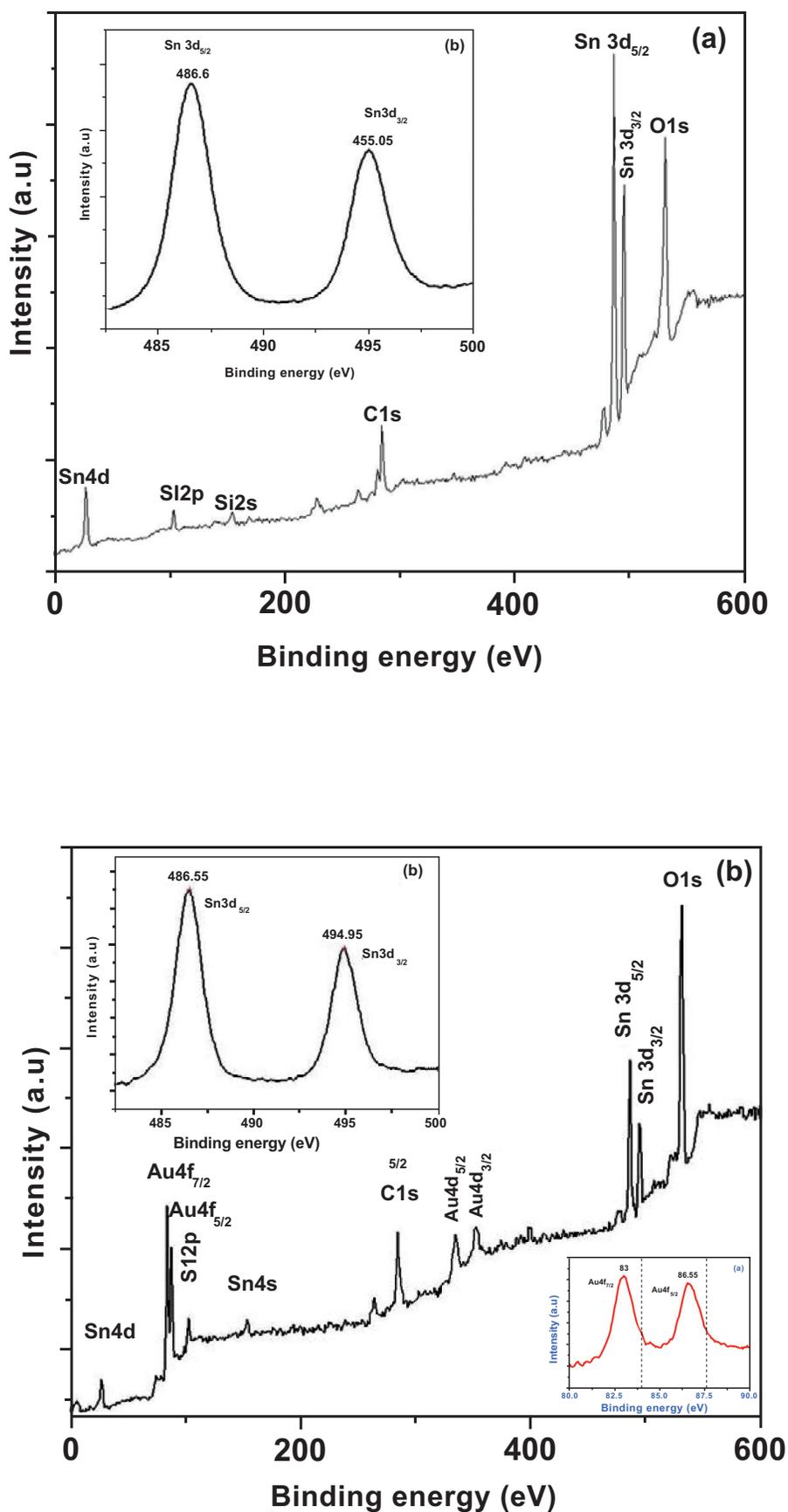
Fig. (3). XPS spectrum of the (**a**) tin-oxide nanoparticles (**b**) Au-SnO$_2$ nanocomposite. The insets show the HRXPS of (**a**) Au4f region, where the dashed lines show the binding energies of bulk gold and (**b**) Sn3d region.

post irradiation with 532 nm and 1064 nm laser wavelength are shown in Fig. (**4**). The absorption spectra of gold colloidal show characteristic surface plasmon absorption peak at 520 nm. The tin oxide colloidal exhibits strong UV absorption and negligible absorption in visible range. The absorption spectra of the sample post irradiated by 1064 nm does not show any appreciable change whereas Au-SnO_2 nanocomposite shows a slight red shift and significant change in the line shape of the plasmon absorption band. The presence of plasmon peak in the spectrum of Au-SnO_2 nanocomposite also confirms the formation of nanocomposite as formation of nano alloy is characterized by a blue shift or complete disappearance of plasmon peak. The absorption results suggest the formation of an intermediate phase upon the nano-joining [21]. This intermediate phase is characterized by a red shift in absorption peak and the position of plasmon peak depends on the size of the synthesized composite nanoparticles. The slight red shift observed in Au-SnO_2 nanocomposite can be ascribed to an increase in particle size upon nano-joining.
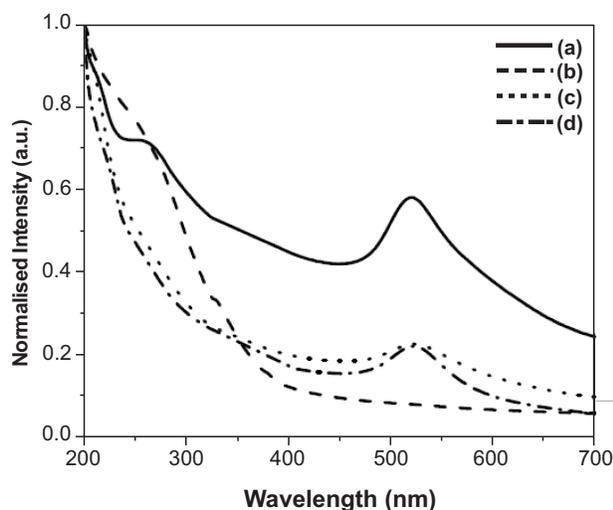
Fig. (4). Optical absorption spectra of (**a**) gold nanoparticles (**b**) tin oxide nanoparticles (**c**) Au-SnO_2 nanocomposite post irradiated by 532 nm (**d**) Au-SnO_2 nanocomposite post irradiated by 1064 nm.

CONCLUSION

We have studied the effect of laser wavelength on the nano-joining process. Our results indicate that nano-joining is a wavelength dependent phenomenon. The formation of Au-SnO_2 nanocomposite by 532 nm laser post irradiation is due to near resonance condition with gold plasmon resonance band. By suitable choice of single component material and laser wavelength PLAL in combination with post irradiation can be used as a convenient synthesis route for the multicomponent materials by nano-joining.

ACKNOWLEDGEMENTS

REFERENCES

[1]   Zeng H, Sun S. Syntheses, properties, and potential applications of multicomponent magnetic nanoparticles. Adv Funct Mater 2008; 18: 391-400.
[2]   Pan X, Fan Z, Chen W, Ding Y, Luo H, Bao X. Enhanced ethanol production inside carbon-nanotube reactors containing catalytic particles. Nat Mater 2007; 6: 507-11.
[3]   Robel I, Bunker B, Kamat PV. Single-walled carbon nanotube–cds nanocomposites as light-harvesting assemblies: photoinduced charge-transfer interactions. Adv Mater 2005; 17: 2458-63.
[4]   Komarnen S. Nanocomposites. J Mater Chem 1992; 2: 1219-30.
[5]   Oldfield G, Ung T, Mulvaney P. Au@SnO$_2$ core–shell nanocapacitors. Adv Mater 2000; 12: 1519-22.
[6]   Yu K, Wu Z, Zhao Q, Li B, Xie Y. High-temperature-stable Au@SnO$_2$ core/shell supported catalyst for CO oxidation. J Phys Chem C 2008; 112: 2244-7.
[7]   Bahrami B, Khodadadi A, Kazemeini M, Mortazavi Y. Enhanced CO sensitivity and selectivity of gold nanoparticles-doped SnO$_2$ sensor in presence of propane and methane. Sens Actuators B 2008; 133: 352-6.
[8]   Yang GW. Laser ablation in liquids: Applications in the synthesis of nanocrystals. Progr Mater Sci 2007; 52: 648-98.
[9]   Tsuji T, Iryo K, Watanabe N, Tsuji M. Preparation of silver nanoparticles by laser ablation in solution: influence of laser wavelength on particle size. Appl Surf Sci 2002; 202: 80-5.
[10]   Dolgaev SI, Simakin AV, Voronov VV, Shafeev GA, Bozon-Verduraz F. Nanoparticles produced by laser ablation of solids in liquid environment. Appl Surf Sci 2002; 186: 546-51.
[11]   Tilaki RM, Iraji zad A, Mahdavi SM. Stability, size and optical properties of silver nanoparticles prepared by laser ablation in different carrier media. Appl Phys A 2006; 84: 215-9.
[12]   Mafune F, Kohno J, Takeda Y, Kondow TJ. Nanoscale soldering of metal nanoparticles for construction of higher-order structures. Am Chem Soc 2003; 125: 1686-897.
[13]   Liang C, Shimizu Y, Sasaki T, Koshizaki N. Synthesis of ultrafine SnO$_{2-x}$ nanocrystals by pulsed laser-induced reactive quenching in liquid medium. J Phys Chem B 2003; 107: 9220-25.
[14]   Buffat P, Borel JP. Size effect on the melting temperature of gold particles. Phys Rev A 1976; 13: 2287-98.
[15]   Takami A, Kurita H, Koda S. Laser-Induced size reduction of noble metal nanoparticles. J Phys Chem B 1999; 103: 1226-32.
[16]   Briggs D, Seah MP. Practical surface analysis 1. Chichester: Wiley and Sons 1990.
[17]   Tian C, Mao B, Wang E, *et al.* Simple strategy for preparation of core colloids modified with metal nanoparticles. J Phys Chem C 2007; 111: 3651-7.
[18]   Arabatzis IM, Stergiopoulos T, Andreeva D, Kitova S, Neophytides SG, Falaras P. Characterization and photocatalytic activity of Au/TiO2 thin films for azo-dye degradation. J Catal 2003; 220: 127-35.
[19]   Arias AC, Roman LS, Kugler T, Toniolo R, Meruvia MS, Hummelgen IA. The use of tin oxide thin films as a transparent electrode in PPV based light-emitting diodes. Thin Solid Films 2000; 371: 201-6.
[20]   Ioannides T, Verykios XE. Charge transfer in metal catalysts supported on doped tio2: a theoretical approach based on metal–semiconductor contact theory. J Catal 1996; 161: 560-69.
[21]   Izgaliev AT, Simakin AV, Shafeev GA, Bozon-Verduraz F. Intermediate phase upon alloying Au–Ag nanoparticles under laser exposure of the mixture of individual colloids. Chem Phys Lett 2004; 390: 467-71.